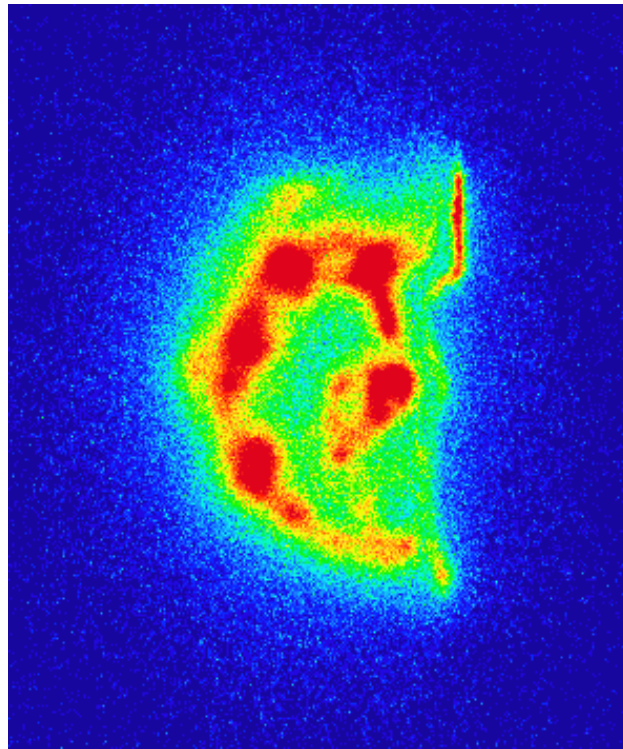




CHALMERS
UNIVERSITY OF TECHNOLOGY



Differentiation of Radionuclides on Surfaces using Autoradiographic Methods

Master's thesis in Nuclear Engineering

ERIK KARLSSON

MASTER'S THESIS 2015:05

Differentiation of Radionuclides on Surfaces using Autoradiographic Methods

ERIK KARLSSON



Nuclear Chemistry
Department of Chemistry and Chemical Engineering
Division of Energy and Materials
CHALMERS UNIVERSITY OF TECHNOLOGY
Gothenburg, Sweden 2015

Differentiation of Radionuclides on Surfaces using Autoradiographic Methods

ERIK KARLSSON

© ERIK KARLSSON, 2015.

Supervisor: Stefan Allard, Department of Chemistry and Chemical Engineering
Examiner: Christian Ekberg, Department of Chemistry and Chemical Engineering

Master's Thesis 2015:05
Nuclear Chemistry
Department of Chemistry and Chemical Engineering
Division of Energy and Materials
Chalmers University of Technology
SE-412 96 Gothenburg
Telephone +46 31 772 1000

Typeset in L^AT_EX
Gothenburg, Sweden 2015

Abstract

This thesis describes work which relates to attempting to obtain quantitative data of radionuclides on surfaces using autoradiography. The main work focuses on introducing shielding in the form of aluminium sheets which attenuate the radiation. In addition a second method was also investigated which was based on summing together the total deposited energy of each impact event registered by the plate separately and comparing it to a set intensity level. The summing method did however not give any useful results other than being able to discriminate between alpha and beta radiation.

The collection of the emitted radiation is performed by a photosensitive plate (Fujifilm BAS-MS) and then turned into useful data by a Fujifilm FLA-7000 scanner. The radiation intensity is quantified in a unit called PSL, which is an arbitrary unit used to describe the absorbed dose of the plate. The measurement of this intensity was made using Fujifilm Image Gauge which gives the total deposited intensity of the sample area. The samples measured were prepared by applying a radionuclide in an acetone solution to a microscope slide. After evaporation the sample was wrapped in a thin plastic film to preserve the integrity of the sample.

The radionuclides focused on in this thesis are ^{85}Sr , ^{134}Cs , ^{152}Eu and ^{63}Ni , although attempts at characterising the nickel had to be discarded due to extremely low emission energies which failed to produce a sufficient absorbed intensity in the plate. For the remaining nuclides a successful characterisation was performed by way of measuring the attenuation. This data was then introduced into a log-plot to find the slope which is the attenuation coefficient.

The attenuation data produced by this method can then be used in a simple equation to give the intensity distribution of a sample (x , and by extension $1 - x = x_2$) given that the attenuation of the sample has been measured ($\mu_{measured}$):

$$\mu_{measured} = x\mu_1 + (1 - x)\mu_2$$

An extension for this method to allow reliable quantification of the actual nuclide content can be introduced by performing a PSL/Bq measurement for the nuclides. Further extension of the method to include more than two nuclides at a time in a mixed sample can be made by performing the shielding experiments with more than one material (n materials allow for quantifying n+1 nuclides).

Keywords: autoradiography, quantification, differentiation, attenuation, shielding, strontium, europium, caesium, aluminium

Contents

List of Figures	viii
List of Tables	ix
List of Images	xi
1 Introduction	1
1.1 Background	1
1.2 Purpose	2
1.3 Scope	2
2 Theory	5
2.1 Imaging plates	5
2.2 Summing approach	6
2.3 Shielding approach	7
2.4 Extending capabilities of the shielding method	9
3 Methodology	11
3.1 Sample preparation	11
3.2 Exposure, scanning and measuring procedure	11
3.3 Summing approach	12
3.4 Shielding approach	16
4 Results	17
4.1 Summing approach	17
4.2 Shielding approach	18
5 Discussion	21
5.1 Summing approach	21
5.2 Shielding approach	21
6 Conclusions	25
6.1 Summing approach	25
6.2 Shielding approach	25
6.3 Future work	26
7 Acknowledgements	29

Bibliography	31
A Appendix 1	I
A.1 MATLAB Code	I

List of Figures

4.1	Plots of ^{85}Sr intensity for different shielding thicknesses (log plot on the right).	19
4.2	Plots of ^{134}Cs intensity for different shielding thicknesses (log plot on the right).	19
4.3	Plots of ^{152}Eu intensity for different shielding thicknesses (log plot on the right).	19
4.4	Plots for the mixed sample of the values in table 4.4, log plot on the right.	20
5.1	Log plot for ^{85}Sr intensity at different shielding thicknesses.	22
5.2	Log plot for ^{134}Cs intensity at different shielding thicknesses.	22
5.3	Log plot for ^{152}Eu intensity at different shielding thicknesses.	22

List of Tables

2.1	Specifications of the two plates used in this work, BAS-SR and BAS-MS.[4]	6
3.1	An example of the output given by the measuring tool of the Fujifilm Image Gauge program.	12
4.1	Measurement values for ^{85}Sr for the different shielding thicknesses.	18
4.2	Measurement values for ^{134}Cs for the different shielding thicknesses.	18
4.3	Measurement values for ^{152}Eu for the different shielding thicknesses.	18
4.4	Measurement values for mixed sample for different shielding thicknesses. ($^{134}\text{Cs}+^{85}\text{Sr}$)	20
5.1	Data for attenuation coefficients of the nuclides as well as uncertainty and fit data.	23
5.2	Data for attenuation coefficients of the mixed sample as well as uncertainty and fit data.	24

List of Images

1	The standard make up of a Fujifilm image plate, simplified into three fundamental layers.	5
2	A single beta count from background radiation, zoomed in (squares are $25 \times 25 \mu\text{m}$, standard SR-plate resolution setting).	7
3	Summation area for a single count, the red square indicates the 7×7 pixel square chosen by the algorithm where the total energy sum is the largest.	13
4	A small piece of the input data directly from the scanner (higher energy background radiation, contrast increased to give a better view).	14
5	Input data with the MATLAB output overlaid on top. The red asterisks are placed where the algorithm found the correct criteria to label the area as a count.	15
6	Raw input data from the scanner, ^{134}Cs on the left, ^{239}Pu on the right.	17
7	Output MATLAB data of the same area as in image 6.	17
8	Fictitious output result from program based on a grid division of the sample space where each grid is measured and given a content value (high resolution).	27
9	Fictitious output result from program based on a grid division of the sample space where each grid is measured and given a content value (low resolution).	28

1

Introduction

This thesis describes work performed to expand the capabilities of the autoradiographic method to include differentiation of nuclides, and by extension quantification. The thesis is written for readers with a basic knowledge of nuclear chemistry.

1.1 Background

Autoradiography is a method to image decay emissions from radioactive nuclides on a surface or in a thin slice of material. This is done by allowing a photographic film or a photosensitive plate to absorb the radiation which stores an image of the absorbed dose in the plate which can be brought out using a scanner.

The autoradiographic method is used most often in biological studies to image the distribution of for example radiolabeled proteins in an organ or other piece of tissue. Historically this has been used to understand mechanisms in cells such as DNA-synthesis and the impact of steroidal hormones as well as mapping out neuronal pathways. Other uses include inspecting metal objects for cracks by injecting a gaseous nuclide, allowing it to diffuse into the material and then imaging it to get a good view of any defects that are present. This is a much more effective method than conventional methods that use dyes to colourise any exposed area which would miss a lot of the smaller cracks.

Autoradiography is characterised by the nuclide being in the material that is being measured. This is the reason for the auto- prefix and it is not to be confused with histo- or microradiography where an external x-ray source is used to produce an image.

The first steps to developing the method were made by Henri Becquerel who noticed that a mysterious emanation from uranium blackened photographic plates, even when an opaque paper was placed in between[1]. This was also the discovery of radioactivity making autoradiography the first radiological method ever used to measure a sample. Later it was also used to make the first characterisations of gamma emissions by Paul Villard who showed that this emission is not affected by magnetic fields using autoradiography.

Autoradiography has accompanied the nuclear field ever since its infancy and it still has a big impact today, a search of the Summon library with the keyword 'autoradiography' yields over 600 journal articles published so far in 2015 (20th of April).

1.2 Purpose

The purpose of this thesis project is to expand the capabilities of the autoradiographic method to include nuclide differentiation. The method is already a powerful tool which can be used to get a good idea of the distribution of nuclides on a surface and to include being able to discriminate between them would further increase its usefulness.

Being able to discriminate between nuclides may enable those who use the method to make assessments regarding the distribution of multiple radionuclides in a sample both qualitatively and quantitatively. This could for example be useful if two radiolabeled proteins (with two different nuclides) are used simultaneously in a sample, or to study how chemical interactions between nuclides influence their distribution and spread during a radiological event.

Knowing the characteristics of the response of the autoradiographic setup to each of these nuclides would then enable the researcher to draw conclusions from the data that they were previously not able to. This opens new possibilities for using autoradiography as a non-destructive measurement method to provide precise results in ways other than just imaging the distribution of activity.

1.3 Scope

The experimental work will be limited to four nuclides commonly used in autoradiography which have the following main emissions [3]:

- ^{134}Cs
A β^- -emitter with emissions over 5% intensity of :
70.19% $\beta_{max} = 658.39$ keV, $\beta_{avg} = 210.3$ keV.
27.27% $\beta_{max} = 89.06$ keV, $\beta_{avg} = 23.2$ keV.

- ^{152}Eu
Decays by electron capture (72.1%) and β^- (27.9%) with emissions over 5% intensity of :
13.8% $\beta_{max} = 695.6$ keV, $\beta_{avg} = 221.7$ keV.
8.17% $\beta_{max} = 1474.5$ keV, $\beta_{avg} = 535.4$ keV.

- ^{63}Ni
A low energy β^- -emitter with emission :
 $\beta_{max} = 66.980$, $\beta_{avg} = 17.434$ keV.

- ^{85}Sr

A pure electron capture nuclide with emission :
(0.0063%) Auger electron : 498.811 keV

The reasoning for only mentioning the emissions above is that they are the emissions expected to be of highest significance with respect to the observed intensity of the image. Some of the nuclides have very low energy β^- -emissions (as well as X-rays) which will not leave a significant signature and perhaps not even make it into the plate itself.

The experimental work regarding shielding is limited to one material, aluminium, which was chosen for its availability both in sheet and foil form as well as it not being completely opaque nor transparent to beta particles. Included in this work is a mathematical background for how additional materials provide further information allowing for more complex measurements.

2

Theory

This section covers the basics of the autoradiographic method as well as the equipment used to perform the experiments. The work in this thesis is based on two different approaches which both are detailed in this section. Also included are physical explanations of the expected effects as well as a mathematical background for how these effects can be used to assess nuclide content in a sample. Finally it is described how the method can be extended to include additional capabilities such as performing content analysis of a sample on more than two nuclides at the same time.

2.1 Imaging plates

The two different plates used for the experimental work of this thesis are the Fujifilm BAS-SR (Super Resolution) and the BAS-MS (Multipurpose Standard) plates. These differ in two ways, the SR plate has a higher resolution and is more suited to precise spatial discrimination whereas the MS plate has a higher sensitivity and is better for work with low activity or low energy nuclides. The imaging plates used are based on the mechanism of exciting a photo-stimulable phosphor (in this case BaFBr:Eu for the SR plate and BaFBr_{0.85}I_{0.15}:Eu for the MS plate)[4] using incident radiation. The plate itself is a flexible 20x25cm sheet made up of several layers that can be described as a support layer, a photo-stimulable layer and a protective coating to prevent damage and wear to the photo-stimulable layer.

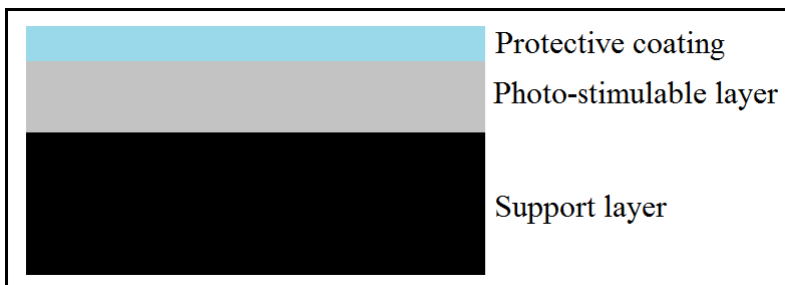


Image 1: The standard make up of a Fujifilm image plate, simplified into three fundamental layers.

The support layer is made out of plastic and an outer layer of a magnetic ferrite compound to hold the plate in place on the scanning cassette.

In the following table data is displayed regarding the makeup of the plates for an easier overview.

Table 2.1: Specifications of the two plates used in this work, BAS-SR and BAS-MS.[4]

Plate type	Pixel size	Dimensions	Phosphor layer makeup
BAS-SR	25 μm	20x25cm	BaFBr:Eu
BAS-MS	50 μm	20x25cm	BaFBr _{0.85} I _{0.15} :Eu

Beyond the differences shown in table 2.1 however the plates work in the same way. The photo-stimulable layer is made up of many crystal grains. These grains are made up of a crystal lattice containing imperfections such as vacancies. The photo-stimulable layer is doped with Eu^{2+} ions which when impacted by an emission become photo-oxidised to Eu^{3+} ions. This also creates electron/hole-pairs where the electrons are now in the conduction band and the holes in the valence band. These electrons are captured by the halogen ion vacancies and the holes are trapped by the europium ions. This creates a retained image in the plate which can be brought out at will by exposing the plate to light. The image is however not permanent and will be subject to fading if scanning is not performed within a reasonable time frame from the completed exposure. This is something which needs to be considered when making longer exposures (days) due to the fading already starting to affect the first registered emission impacts while the plate is still being exposed.

When the plate is later exposed to visible light, during scanning or otherwise, the electrons are freed from the vacancies. They are then returned to the conduction band which reduces the europium ions into excited Eu^{2+} ions that in turn emit light upon de-excitation which is picked up by the scanner to produce an image. These processes all have energy level differences on the order of a few electron volts giving a good energy resolution for the emissions deposited in the plate.[2]

The image is registered by a computer program (Fujifilm Multi Gauge[5]) which displays it along with a broad toolbox to adjust brightness and mark out areas of interest. The program is also able to measure the total deposited energy of an area while simultaneously adjusting for the background giving an accurate value of the deposited energy from the sample.

2.2 Summing approach

The initial attempt to differentiate nuclides was made by looking at each count and its properties individually. Since the deposited energy in the plate is directly proportional to the incident energy of the radiation you can make some observations. The unit used for measuring the deposited energy is the arbitrary unit PSL (photo-stimulated luminescence). An example of a definition which puts it into perspective

is as follows: "An 80 kV tungsten target X-ray source of $3.8 \cdot 10^{-8} \text{ A s kg}^{-1}$ yields a value of 100 PSL/mm^2 for standard imaging plate Fuji model SR." [7]

The summing approach was based on a program written in MATLAB (Appendix A.1) which takes the raw data from the autoradiograph scanner and processes it. This processing is in effect a summation of the energy deposited by the interaction of the emission and the plate since it is not confined to a single pixel. The following is an example of how a single such event is displayed in the scanned image:

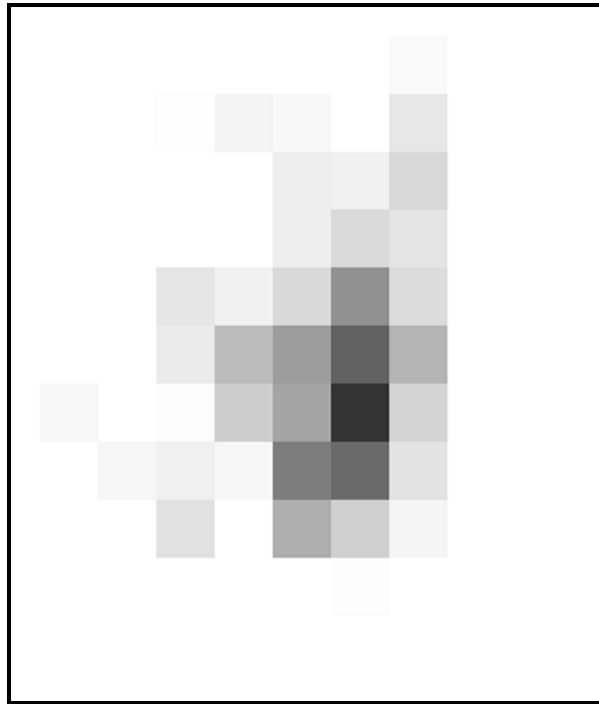


Image 2: A single beta count from background radiation, zoomed in (squares are $25 \times 25 \mu\text{m}$, standard SR-plate resolution setting).

As can be seen in image 2 the count is spread out over a neighbourhood of pixels which means that these pixels need to be summed to give a total deposited PSL-value for the count. The grey level of the pixels is indicative of the total absorbed energy of that spot on the plate (darker means more absorbed energy).

2.3 Shielding approach

The shielding approach is based on the concept of attenuation of radiation by introducing a shielding material. This can be used to characterise different energies or types of radiation as they are attenuated differently when interacting with a material. When differentiating nuclides in this manner what you are looking for is a signature attenuation for the nuclide which is not applicable to any one emission (unless the nuclide has a single mono-energetic form of decay). The attenuation is a sort of sum of all the different effects on the radiation when interacting with the

2. Theory

shielding material. The method of shielding makes use of this sum of effects who all influence the attenuation coefficient of the nuclide.

This approach is centred on this equation describing the fall-off of radiation intensity as the shielding material gets progressively thicker :

$$I = I_0 e^{-\mu d} \quad (2.1)$$

Where I_0 is the unshielded intensity, d is the shielding thickness, μ is the attenuation coefficient and finally I is the shielded intensity. The μ for a particular nuclide depends on the β_{max} energy (or energies) as well as other emissions such as x-rays, gamma emissions and Auger electrons. Due to all these effects, nuclides have quite varied attenuation coefficients and this can be used to differentiate them. When more shielding material is added gradually you get a different decrease in total absorbed energy in the plate for different nuclides, given that their emissions are not very similar (for example two β -nuclides that are very close in β_{max} energy would not be appropriate for this method). By utilising this difference you can characterise how nuclides behave when shielded by a certain shielding material. This information can then be used to determine the nuclide content of a sample by observing how the total intensity of the sample is reduced when shielding material is added.

If a sample consists of more than one nuclide, the observed attenuation will be a weighted mean between the attenuation behaviours of the nuclides by themselves. If your observed sample attenuation coefficient is μ_{sample} and you know the attenuation coefficients of the pure nuclides the contents of the sample can be calculated as follows :

$$\mu_{sample} = (1 - x)\mu_{N1} + x\mu_{N2} \quad (2.2)$$

The known attenuation coefficients for nuclide 1 and 2 (μ_{N1}, μ_{N2}) in equation 2.2 are the ones determined by experiment. From this you can then rearrange the equation to give the absorbed energy fraction of nuclide 2 as "x".

$$x = \frac{\mu_1 - \mu_s}{\mu_1 + \mu_2} \quad (2.3)$$

This information given by equation 2.3 can then be converted into nuclide content by making measurements regarding what the PSL/Bq-value is for that particular nuclide.

2.4 Extending capabilities of the shielding method

In this work the shielding method is confined to working on just two nuclides as there is not enough information to make an assessment of more than that at a time. However the method can be expanded by performing measurements on more than one material for shielding. The prerequisites for this to work is that the attenuation behaviour for the materials needs to not be too similar if an accurate value for the nuclide content is required. For two materials you can perform the method on three nuclides simultaneously using the following equations :

$$\mu_{sample}^{M1} = \mu_1^{M1}x_1 + \mu_2^{M1}x_2 + \mu_3^{M1}(1 - x_1 - x_2) \quad (2.4)$$

$$\mu_{sample}^{M2} = \mu_1^{M2}x_1 + \mu_2^{M2}x_2 + \mu_3^{M2}(1 - x_1 - x_2) \quad (2.5)$$

M1 and M2 denote the two shielding materials, $\mu_1^{M1}, \mu_2^{M1}, \mu_3^{M1}$ are the attenuation coefficients for the first material and the ones denoted M2 are for the second material. All those values are known and along with the measured attenuation for the samples with the two materials ($\mu_{sample}^{M1}, \mu_{sample}^{M2}$) we now have two equations (2.4, 2.5) with two unknowns (x_1, x_2) meaning we can solve the system for these absorbed energy fractions. This can be extended further as you will always be able to do measurements on $n+1$ nuclides when n number of materials are used. However, it might be difficult to obtain materials where the attenuation characteristics are different enough to be able to provide good values.

3

Methodology

3.1 Sample preparation

Two kinds of samples were prepared for this work as the requirements for the two methods were quite different. The shielding approach samples were prepared by using a solution consisting of acetone spiked with a nuclide. This solution was prepared by taking a 10 mL vial of acetone and spiking it with the nuclide in amounts which would yield an end result of an activity of roughly 100 kBq/ml. This was decided on to avoid handling large amounts of activity but at the same time be able to keep the exposure time at a reasonably low level. From this solution a volume of 0.1 mL was taken using a pipette and applied to the centre of a glass microscope slide. The solution was allowed to evaporate and the slide was marked with identifying information to avoid later confusion. Also applied was a small plus-sign in the top left corner to keep track of which side of the slide the nuclide was applied to. To avoid the nuclide rubbing off when performing experiments the slides were also wrapped in plastic to seal the nuclide. The summing approach samples were prepared in the same way but the activity was much lower (roughly 10-15 Bq in the sample) to get a good separation of the counts on the plate to allow for analysing them individually.

3.2 Exposure, scanning and measuring procedure

The exposures were performed by first erasing an imaging plate in the eraser[6], a machine which works by illuminating the plate with bright visible light to make sure the plate has no stored image. This is necessary because the scanning procedure is sometimes not sufficient to fully clear the plate. Another factor to consider is also that the plate accumulates background radiation from the moment it is taken out of the eraser which can interfere with the measurement. To avoid this it is recommended that the plate is removed from the eraser just before exposing to minimise this effect.

When the plate is sufficiently erased it is placed on a surface where after a plastic film (Gladpak was used for this work) is applied to the imaging plate to protect it from mechanical damage as well as contamination from the sample. The nuclide

samples are then placed on the plate which is then enclosed in the exposure box, a box made of plastic designed to keep out ambient light (as well as some background radiation) during the exposure which would otherwise affect the results. After the exposure is done the box is removed and the nuclides are taken off the plate. The plate is placed on the scanning cassette which is then placed in the scanner, this needs to take place right after the exposure due to the accumulation of background radiation in the plate.

For the summing approach the measuring procedure was very minimalistic in that the raw data was exported directly from the scanner into MATLAB without performing measurements. The shielding approach results however were based on the measurements made in the Fujifilm Image Gauge program provided with the scanner. In this program the raw scanning data was imported and the brightness and contrast was increased to near maximum values. This gives a better view of the deposited energy since the program otherwise normalises what it displays which might lead to the user selecting a too small area for measuring. When the image has been processed to correctly display the exposed areas a selection is made which includes all of the exposed area. If more than one sample is being measured at the same time, the selections are made separately. Finally a non-exposed area is selected which contains only background radiation, this is done to be able to correct the exposed areas for background radiation content.

The program then produces an output of how many total PSL units the areas contain, this is directly related to the absorbed energy of the area. An example of the output of the program looks like this:

Table 3.1: An example of the output given by the measuring tool of the Fujifilm Image Gauge program.

Region	Area (mm ²)	PSL	PSL-BG	BG	PSL/mm ²
1	1502.5	115678.2	112222.45	3455.75	76.99
2*	467	1074.1	0	1074.1	2.3

The region given as '1' is the sample and the '2*' is the background radiation area. The important value to look for in this measurement is the PSL-BG value which is the PSL value with the background radiation removed. This is the value used in the calculations as it is directly related to the absorbed energy.

3.3 Summing approach

To get the full PSL value of the count a summation area had to be decided on, one that was large enough to cover a whole count but still small enough to not accidentally sum two counts into one. The example count shown in image 2 has a

very standard appearance with regard to other observed counts and by assessing the spatial distribution of it an area of 7x7 pixels was decided on. What the process of summing does is that it takes an area of 7x7 pixels centred on the pixel in question and sets this as the new value of the pixel before it moves on to the next pixel (this is done on a separate matrix to not affect the values which are being summed). The area of summation for a single count is depicted below :



Image 3: Summation area for a single count, the red square indicates the 7x7 pixel square chosen by the algorithm where the total energy sum is the largest.

As can be seen in image 3 the summation is not necessarily centred on the count but is instead placed so the maximum PSL value possible is included in the summation. Before doing the summation however the raw data from the scanner had to be converted into the correct format. The data provided from the scanner has a QL (quantum level) value for each pixel which is related to the PSL-value by the following formula given by Fujifilm documentation [8]:

$$PSL = \frac{P_s^2}{100} \cdot \frac{4000}{S} \cdot 10^{L \cdot \frac{QL}{65535} - 0.5} \quad (3.1)$$

P_s = pixel size = 25 (25 μ m)

S = sensitivity = 10000

L = latitude = 5

QL = quantum level input from raw data

The number 65535 is related to the bit-value of the image ($16, 2^{16} - 1 = 65535$)

Feeding the image pixel by pixel into the formula above produces a new image with PSL-intensities instead of quantum levels provided for each pixel. This image is fed into a MATLAB program (Appendix A.1) which performs the summation described above. After the summation the summed values are sorted by size and the largest one has its position recorded in two vectors (x and y position). To prevent a count being registered twice, by for example the side of a count exceeding the set PSL-value limit a padding has to be performed on each count after it has been recorded. This was done by setting all grey values within a 10 pixel radius from the count to zero before doing the previously described iteration of summation and sorting all over again.

When the program no longer finds any points exceeding the PSL limit the x and y positions from the vectors are plotted producing an image of the spatial distribution of the counts. An example of such an output along with the input image used to produce it is shown below:

Input image:

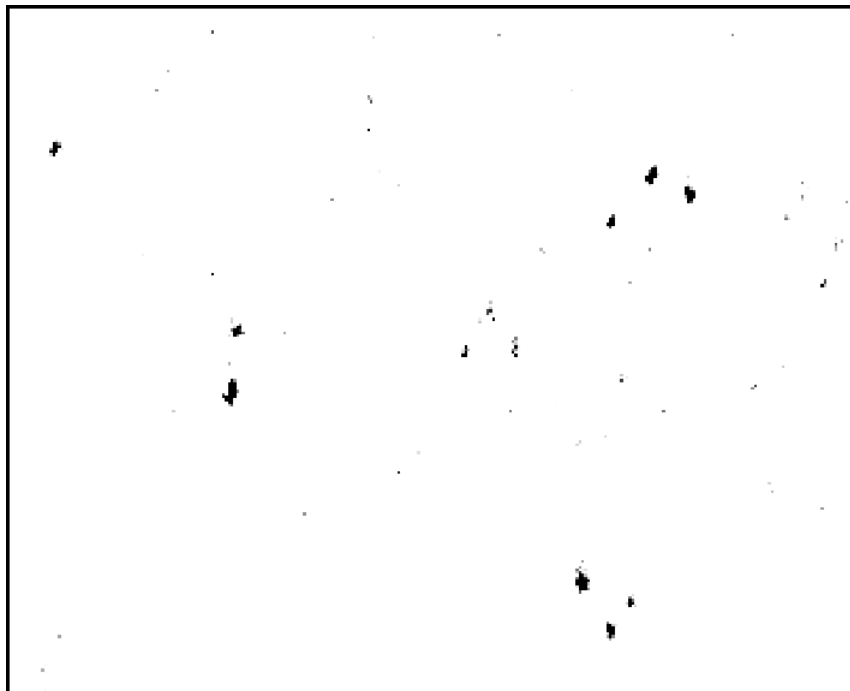


Image 4: A small piece of the input data directly from the scanner (higher energy background radiation, contrast increased to give a better view).

Processing this image in MATLAB gives the x and y values for the counts fulfilling the criteria set by the user (in this case $PSL > 0.04$) and overlaying it with the raw data gives this result:

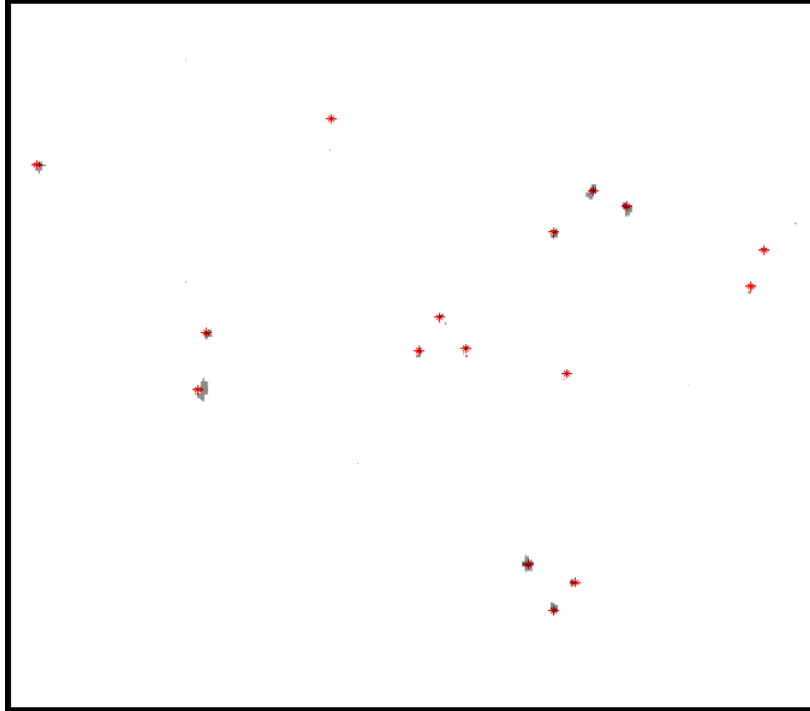


Image 5: Input data with the MATLAB output overlaid on top. The red asterisks are placed where the algorithm found the correct criteria to label the area as a count.

The reasoning for the set PSL-value limit was to look at the distinct counts, sum the values and see in what range we usually end up. This method coupled with data from C.J. Zeissler and A.P. Lindstrom[7], decided on a value of 0.02 PSL per count to qualify it as a proper count. Lower PSL values, such as those deposited by low energy beta radiation are also shared with a significant amount of background noise. Using a value lower than 0.02 would result in false counts being registered due to low-energy noise from background radiation as well as imperfections in the scanning process. There is of course some uncertainty involved in choosing the limit value for this, however a small change in this value does not impact the results in any significant way.

3.4 Shielding approach

The second approach to be tried in this work was to introduce shielding in the form of aluminium to examine how the nuclides attenuate when the thickness is gradually increased. First the nuclides were measured without shielding to get a baseline PSL value for the set measurement period of 30 minutes. This time was decided on by first doing measurements on repeatability and linearity of the dose/PSL response. What these measurements showed was that at PSL/sample values of less than 100000 PSL the repeatability of the experiment was not sufficient. For nuclides that did not exceed this value for the measurement time, a longer measurement time was used where after the PSL/sample value was normalised for a 30 minute measurement. As the shielding thickness was increased the exposure times also went up due to the intensity being attenuated more and more.

When a sufficient number of data points had been obtained for a nuclide, a log plot was made which for the equation stated previously (2.1) is a straight line with slope μ . To find this slope a linear estimate was made in Excel using the LINEST function. This was done with a two sigma confidence (95%) which initially gave a quite large confidence band. To combat this additional data points were generated in Microsoft Excel 2013 using a mean along with a calculated standard deviation for both the absorbed energy and the shielding thickness. These deviations were estimated to be $\pm 0.01\text{mm}$ for the shielding thickness. The uncertainty for the absorbed energy was set to $\pm 1\%$ based on own previous studies regarding reproducibility as well as the uncertainties in the exposure time. The data points were generated using a normal distribution which was considered valid because of a well-established standard deviation. This greatly reduced the two sigma interval for the slope and thus the uncertainty for the measured nuclide content in the sample.

4

Results

4.1 Summing approach

The useful data from this method was limited to differentiation between beta and alpha counts which the following images are an example of. The first image is the raw input data from the scanner where an area of beta counts has been artificially placed next to an area of mostly alpha counts using the cut and paste tools. This data was then fed into the MATLAB program made to differentiate between the counts yielding the following results:

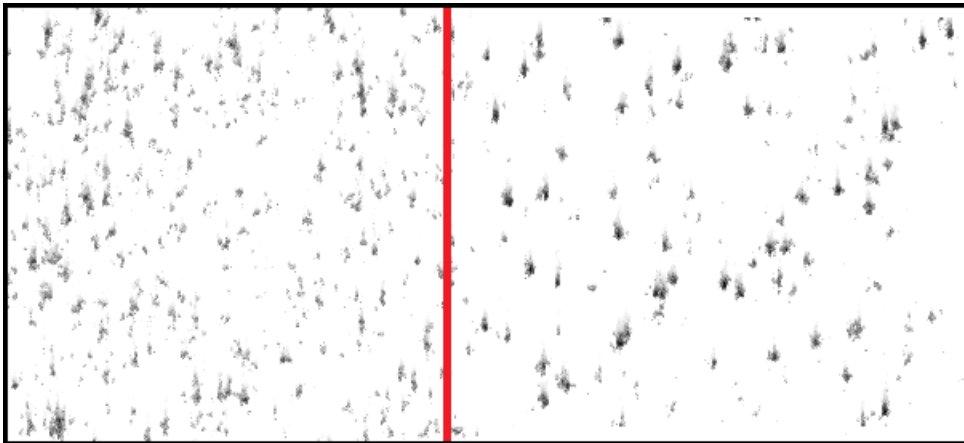


Image 6: Raw input data from the scanner, ^{134}Cs on the left, ^{239}Pu on the right.

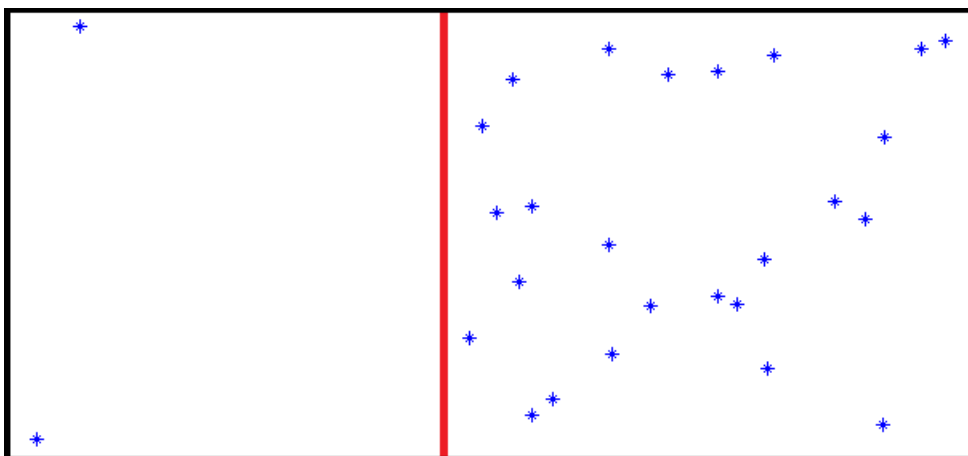


Image 7: Output MATLAB data of the same area as in image 6.

By looking at images 6 and 7 one can see that the algorithm is quite adept at distinguishing between alpha and beta counts, although some overlapping beta counts do register as alpha. (The red line was added manually as a visualisation aid for the reader.)

4.2 Shielding approach

Following in this section are the results from the study of the attenuation coefficients of the nuclides. On the left in each table is the thickness of the aluminium shielding used to measure and on the right is the output PSL per sample value (corrected for background) from Fujifilm Image Gauge. The PSL values have also been corrected for the measured uncertainty which is given next to each value ($\pm 1\%$).

Table 4.1: Measurement values for ^{85}Sr for the different shielding thicknesses.

^{85}Sr	
Shielding thickness	PSL
0 mm	440000 ± 4400
0.3 mm	140000 ± 1400
0.5 mm	65000 ± 650
1.07 mm	57000 ± 570
2.04 mm	45000 ± 450
3.14 mm	41000 ± 410

Table 4.2: Measurement values for ^{134}Cs for the different shielding thicknesses.

^{134}Cs	
Shielding thickness	PSL
0 mm	240000 ± 2400
0.096 mm	110000 ± 1100
0.3 mm	29000 ± 290
0.5 mm	11400 ± 1140
0.77 mm	5600 ± 56

Table 4.3: Measurement values for ^{152}Eu for the different shielding thicknesses.

^{152}Eu	
Shielding thickness	PSL
0 mm	157000 ± 1570
0.3 mm	110000 ± 1100
0.5 mm	83000 ± 830

Plots (with a log plot side by side) of the values in tables 4.1, 4.2 and 4.3 for the different nuclides :

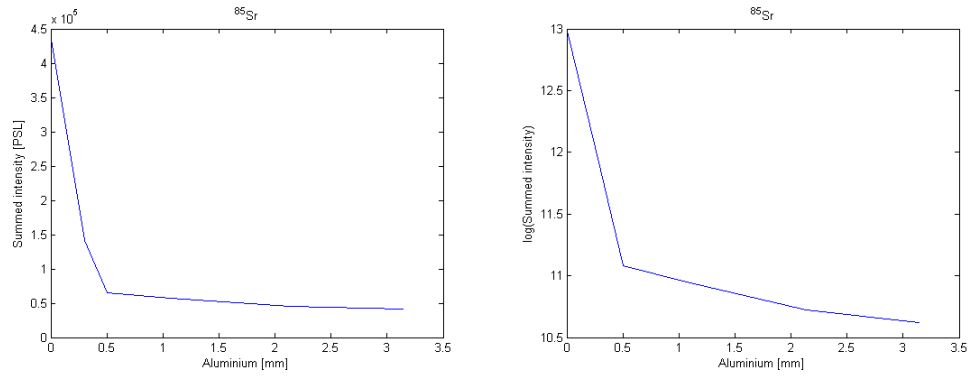


Figure 4.1: Plots of ^{85}Sr intensity for different shielding thicknesses (log plot on the right).

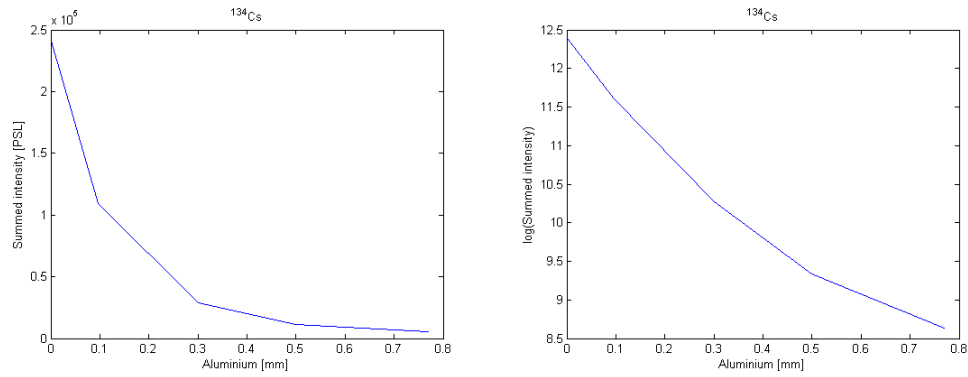


Figure 4.2: Plots of ^{134}Cs intensity for different shielding thicknesses (log plot on the right).

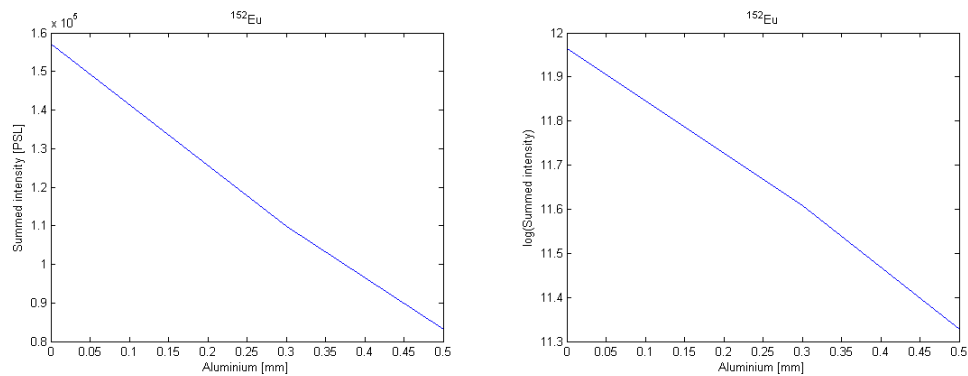


Figure 4.3: Plots of ^{152}Eu intensity for different shielding thicknesses (log plot on the right).

4. Results

Also tested was a mixed sample of ^{134}Cs and ^{85}Sr giving the following table and plots :

Table 4.4: Measurement values for mixed sample for different shielding thicknesses. ($^{134}\text{Cs}+^{85}\text{Sr}$)

Mixed sample.	
Shielding thickness	PSL
0 mm	450000 ± 4500
0.3 mm	116000 ± 1160
0.5 mm	54000 ± 540

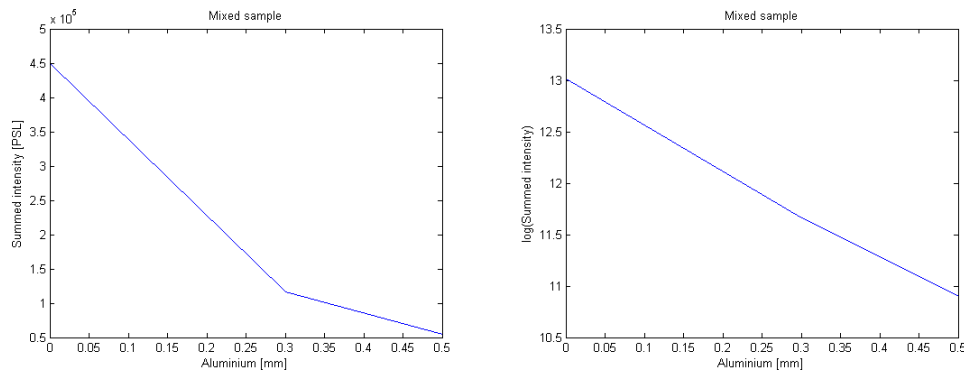


Figure 4.4: Plots for the mixed sample of the values in table 4.4, log plot on the right.

5

Discussion

5.1 Summing approach

This method was as demonstrated a good tool to pick out high energy counts from a low energy background, but failed at being able to distinguish beta decaying nuclides from each other. Mainly this was due to the beta particles not depositing all their energy in the plate but instead having a propensity to scatter. Another problem was due to the continuous spectrum of decay energy a reliable PSL limit value could not be set to differentiate two nuclides since most of the counts would overlap in PSL/count-values.

The only case where the method was somewhat useful was when distinguishing between beta and alpha counts. This was mainly due to the large difference in the PSL/count-value as well as the alpha counts not having the same tendency to scatter or pass through the plate without depositing their full energy which is something the beta particles did. Figure 2 is an example output from the MATLAB code when presented with two areas, one with beta counts from a ^{134}Cs sample (left) and the other with counts from a ^{239}Pu sample (right). The PSL/count limit is set at 0.044 which was settled on by manually counting the value for a plutonium count.

As can be seen, the method is fairly reliable for finding which counts are alpha counts but it does still miss some counts and yield false positives for others due to counting two counts as one.

5.2 Shielding approach

To properly interpret the data gathered using the shielding approach we first have to figure out what is needed. The experiment is an attempt to differentiate nuclides based on the difference in their behaviour when shielding is added between the sample and the imaging plate. To do this we need to look at a parameter and figure out where and why it is differing. From examining the log-plots in the results section we can see that in the strontium graph (also somewhat in the caesium), the slope is varied depending on where in the figure we look. This is due to there being several sources of radiation from these nuclides and the response to shielding from them is very different. To combat this intervals have been chosen for the nuclides where the

behaviour indicates a linear response to shielding due to no emission being blocked sufficiently to alter the slope of the graph. One can compare this to looking at a decay curve (counts vs time) for several different nuclides at the same time, in that case the slope also changes as time progresses. By using this method with the intervals settled on, these plots were produced:

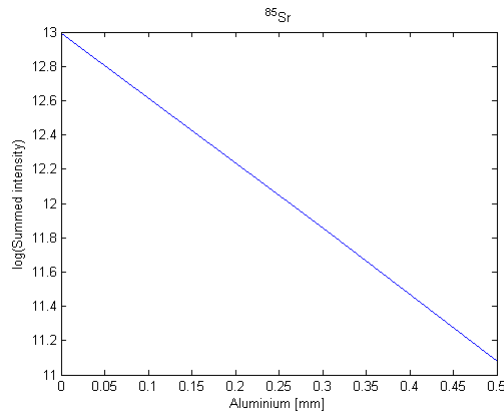


Figure 5.1: Log plot for ^{85}Sr intensity at different shielding thicknesses.

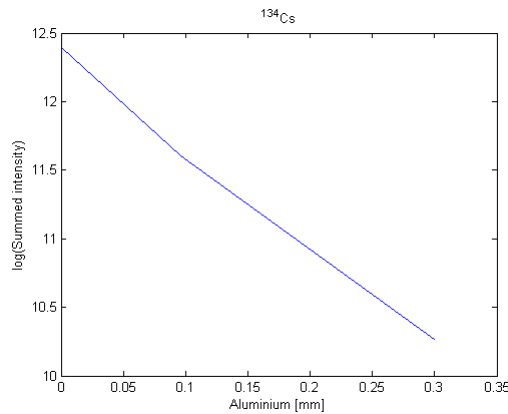


Figure 5.2: Log plot for ^{134}Cs intensity at different shielding thicknesses.

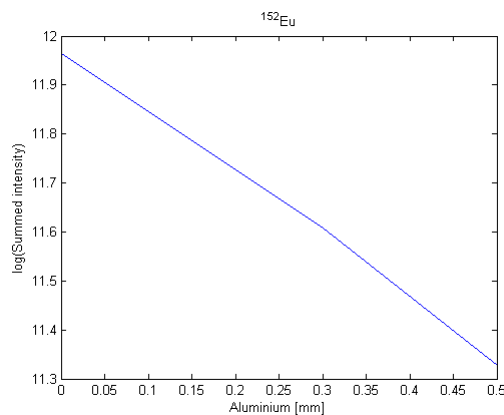


Figure 5.3: Log plot for ^{152}Eu intensity at different shielding thicknesses.

The figures 5.1, 5.2 and 5.3 contain three values each for the aluminium thickness which yields quite a large value for the uncertainty when doing a confidence interval calculation. To combat this more points were generated as described in the 'Methodology'-section. When these points were included in the data set and subjected to a linear estimation the following data was produced :

Table 5.1: Data for attenuation coefficients of the nuclides as well as uncertainty and fit data.

^{85}Sr	
μ	-3.81
Uncertainty	0.03
R^2	0.9981
^{134}Cs	
μ	-7.05
Uncertainty	0.098
R^2	0.9946
^{152}Eu	
μ	-1.26
Uncertainty	0.017
R^2	0.9945

From this it can be seen that the attenuation coefficients for the nuclides are very different indeed, which was a prerequisite for the viability of the method. To further expand on the accuracy the confidence intervals for these values were calculated to be within 0.5% of the values in the table using the excel function CONFIDENCE.NORM with the given uncertainties and a data set size of 30 points.

As a test of how the method would work in a mixed sample, a mix of ^{85}Sr and ^{134}Cs was prepared on a slide by the same method described in methodology to see how it behaved when shielding material was added. The results fit the expected outcome of the sample having an attenuation coefficient between the one for strontium and the one for caesium. The mixed sample was prepared originally to have the same amount of beta emissions from the strontium and the caesium however the strontium also has several other kinds of emissions which contribute to the intensity. This led to the mixed sample being quite heavy in strontium which can also be seen in the data as the slope is much closer to the strontium slope.

Table 5.2: Data for attenuation coefficients of the mixed sample as well as uncertainty and fit data.

$^{85}\text{Sr} + ^{134}\text{Cs}$	
μ	-4.23
Uncertainty	0.056
R^2	0.9951

By using the calculation from the 'Theory' part along with the values for the mixed sample the distribution of deposited energy between ^{85}Sr and ^{134}Cs can be produced as follows:

$$3.81x + (1 - x)7.05 = 4.23 \Rightarrow x = \frac{4.23 - 7.05}{3.81 - 7.05} = 0.870 \quad (5.1)$$

We can say that 87.0% (with a 5.8% uncertainty from error propagation in the equation) of the deposited energy is from the strontium with the remainder being from the caesium. The uncertainty due to error propagation makes the total uncertainty grow quite a bit from the original values which have a maximum uncertainty of 1.4% (in the caesium case). This uncertainty could be brought down by using shielding which has a more precisely defined thickness, as well as reducing the variation of the measuring time. Additional tests have to be made to determine the content of the sample, such as determining the PSL/Bq value of the two nuclides.

6

Conclusions

6.1 Summing approach

The summing approach proved to be a fairly powerless tool in accomplishing the set purpose of this thesis. It requires a very low activity as well as activity ratios between the nuclides which are of comparable orders. The measuring times have to be very short to not allow any sort of overlapping impacts and if the emissions of the two nuclides are similar it is hard to draw any conclusions. As mentioned before in this thesis the problem with beta emissions is that they are continuous in energy over a large bound which statistically makes it very unlikely for two beta emissions from the same nuclide to be of the same energy. The other part of the beta decay, the neutrino, of course continues on through the plate (and likely the whole planet earth) giving no contribution to the intensity. Even if you have two beta particles of the same energy it is very unlikely that they will have the same angle of incidence or that they will both leave all of their energy in the plate without scattering off it or passing on through it.

The only real results from the summing approach was that it can tell apart alpha and beta radiation, as long as the beta radiation is not of very high energy. This can however not be done quantitatively and a qualitative assessment on the nature of the radiation is possible using the naked eye anyway rendering the method unviable.

6.2 Shielding approach

This approach initially showed no promise to be an efficient tool in determining the nuclide content of a sample. During the first experiments repeatability was shown to be a huge issue due to the plates having a non-linear dose response at low doses. This made it impossible to make any conclusions since the deposited energy varied by a factor of 1.5 between the same measurements being performed. After increasing the strength of the samples used, a high repeatability with a low uncertainty was achieved. The uncertainty mostly comes from the difference in time for the measurement as well as only recording what day the samples were prepared. For example, including hours would make a slight difference for the strontium due to it having a fairly short half-life (~ 60 days).

Some of the constraints of the summing approach do appear here as well, such as that there needs to be a sufficient variation in the characteristics of the radiation that is emitted. It does not necessarily have to be just in energy, it can also be in what is emitted and how often.

The method itself might seem a bit time consuming as the measurements have to be repeated with different thicknesses but with regard to its precision it is the only reliable non-destructive method with these capabilities. If you have markers in your sample which you can reliably use as references the method also becomes a powerful tool with regard to determining the spatial distribution in detail as you can now measure a fixed area instead of the whole sample in Image Gauge.

Measurements performed to characterise the nuclides with respect to their attenuation coefficients can be reused as references for all samples containing these nuclides (given that the same plate and scanner are used). However, one must also consider the possibility of self-attenuation in the sample or other losses and leaks of energy.

6.3 Future work

Extending the capabilities of the methods described in this thesis is quite straightforward. To increase the versatility and usability of the method the shielding approach can be extended to utilise more materials. This would as described in the theory section make it possible to do measurements on more than two nuclides at once, the limiting factor being only how different they are with respect to their attenuation coefficients in the materials. One would although still have to know what nuclides the sample contains to be able to perform a successful analysis.

Another point brought up in this thesis where it would benefit from future work is in the translation of deposited energy fraction to nuclide content. This value would be a measurement on how many PSL you get for a set amount of Bq of a nuclide over a set amount of time, a sort of PSL/count value. Because of the nature of beta-emitting nuclides and the continuous energy spectrum of the beta emission you would have to measure for a sufficient amount of time to get a good average for this value. To get a value which is useful the measurements for this need to be performed using the same kind of plate and scanner that are later used to perform the nuclide content measurements. This is because there are significant differences in how many PSL you would get for a fixed nuclide content for an MS plate and an SR plate. This measurement would have to be done only for the nuclide that is of interest. For example if a sample containing caesium and strontium is measured and you have the total PSL value plus the deposited energy fraction you can translate how much of the energy is from one nuclide. This along with the PSL/count value can then be used to get the nuclide content.

To automate the process one could for example write a program which makes the measurements otherwise performed in Fujifilm Image Gauge. For a precise result with regard to the spatial distribution the sample space could be divided into a grid where each node of the grid is measured as if it was an individual sample. This would give a low resolution image of the distribution that still has enough information to draw conclusions from. The following image is an example of how such a result would look with a high resolution grid and three samples (^{85}Sr , mixed sample and ^{134}Cs):

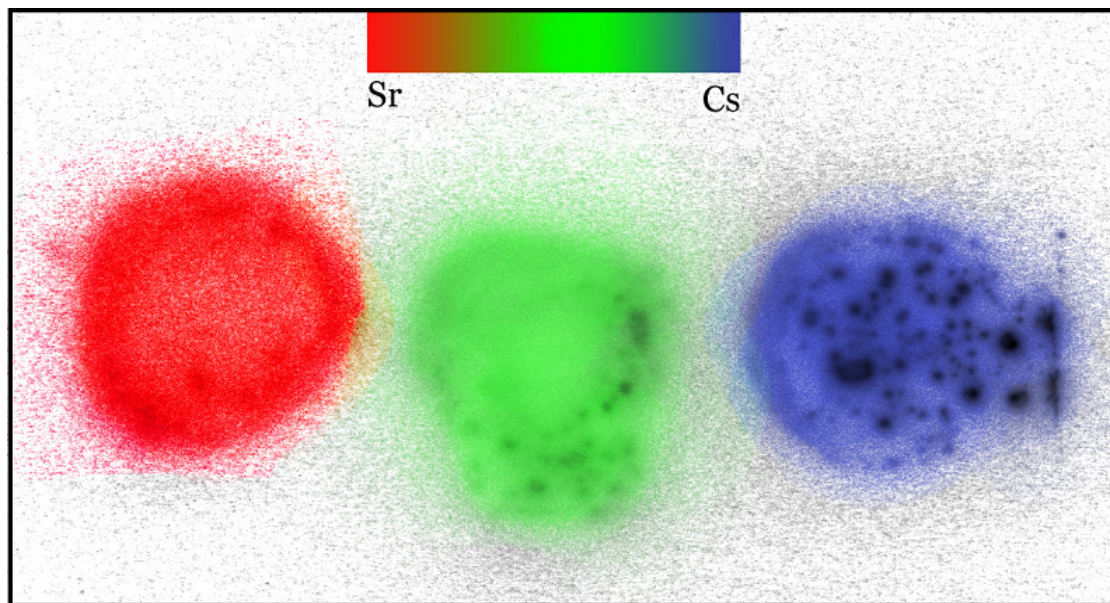


Image 8: Fictitious output result from program based on a grid division of the sample space where each grid is measured and given a content value (high resolution).

To make such a result possible it would necessitate that the samples are held in the same place on the imaging plate during all the measurements to make sure they stay in the same arrangement. This is imperative when multiple measurements are performed if an accurate result is desired.

In image 8 the grid is of a very high resolution but with a more conservative approach it would probably be limited to a grid with sides of at least a few millimetres. Limiting factors in this method are introduced by the leakage of radiation from one sample node to another. If a node contains a high amount of the nuclide which has a lower attenuation coefficient the radiation from that nuclide will leak into adjacent nodes giving an artificially reduced attenuation coefficient. The program will then interpret this as the adjacent nodes having a higher content of that nuclide than what is actually the case. To combat this the grid size has to be increased however the effect is never completely avoidable. A more realistic grid size is depicted in the following image:

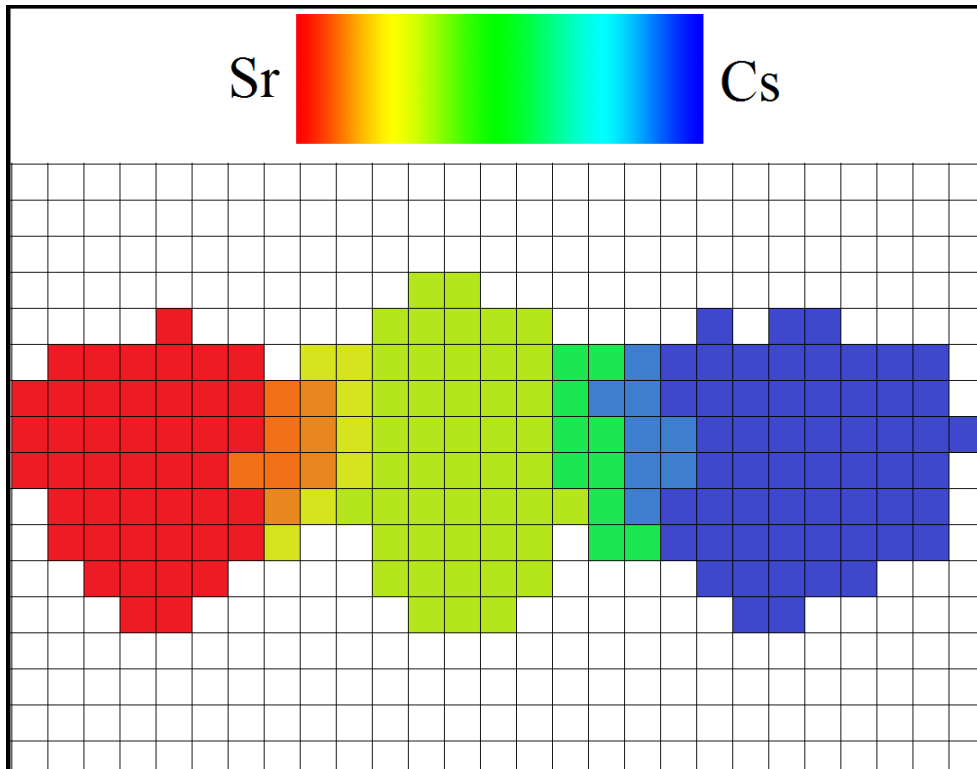


Image 9: Fictitious output result from program based on a grid division of the sample space where each grid is measured and given a content value (low resolution).

This image is of a much lower grid resolution but still it gives a good indication of the nuclide distribution in the sample. A final realistic limit for the resolution of such a measurement would probably fall somewhere between the ones depicted in image 8 and image 9.

7

Acknowledgements

I would like to thank my supervisor Stefan Allard for being a valuable resource to ask questions in times of need and for being helpful and giving suggestions on how to proceed. I would also like to thank Stellan Holgersson for being accessible whenever I needed to prepare samples, Henrik Ramebäck for being interested and attempting to help me figure out why my data did not agree with what was predicted and Christian Mila for providing the materials needed for the work and a proper workstation. Lastly I would like to thank Teodora Retegan for providing valuable support and input throughout the entirety of the work.

Erik Karlsson, Gothenburg, May 2015

Bibliography

- [1] M F. L'Annunziata (2012) Handbook of radioactivity analysis p.1210
- [2] M. Hareyama, N. Tsuchiya, M. Takebe and T. Chida (2000) Two-dimensional measurement of natural radioactivity in granitic rocks by photostimulated luminescence technique. *Geochemical Journal*, Vol. 34, pp. 1 to 9
- [3] E. Schönfeld, R. Dersch (2004) *Table de Radionucléides*
- [4] A. L. Meadowcroft, C. D. Bentley, E. N. Stott. (2008) Evaluation of the sensitivity and fading characteristics of an image plate system for x-ray diagnostics. *Review of Scientific Instruments*, Volume 79, Issue 11 Table I.
- [5] Fuji Photo Film Co. Ltd. Science Systems. (2002) *Science Lab 2002, Multi Gauge Ver 2.0 Operation Manual*
- [6] Fuji Photo Film Co. Ltd. Science Systems. (1998) *FLA-3000 User Manual*.
- [7] C.J. Zeissler, A.P. Lindstrom. (2010) Spectral measurements of imaging plate backgrounds, alpha-particles and beta-particles. *Nuclear Instruments and Methods in Physics Research Section A: Accelerators, Spectrometers, Detectors and Associated Equipment*, Volume 624, Issue 1, pp 92. to 100
- [8] Fuji Photo Film Co. Ltd. Science Systems. (2003) *Image Format Description, BAS2500 system*.

A

Appendix 1

A.1 MATLAB Code

```
A = analyze75read('betaalpha') \ %Read data from Fujifilm Image Gauge
A=rot90(A,3) %Rotate data to correct position
A=flipud(A); % Flip
%%
A=(25./100).^2.*(4000./10000).*10.^(5.*(A./(2^16)-0.5)) %Convert QL to PSL
%%
B=ones(7); % Create summing matrix
s=conv2(A,B,'same') %Make summed matrix s where each value s(x,y)
                    %is the sum of the 7x7 pixel square centered on s(x,y)
%Finding counts
i=1; %Set counter
maxval=10;
while maxval>0.044 %Check if the PSL value is high enough to represent a count

[maxval maxloc] = max(s(:)); %Find the location and value of max(s)
[x y] = ind2sub(size(s), maxloc); %Save the location of the value
countsax(i)=x; %Save X position of count i
countsay(i)=y; %Save Y position of count i
pslvaluea(i)=maxval; %Save PSL value for count i
i=i+1 %Increment counter
for paddery=0:10
    for padderx=0:10
        if x+padderx<(length(s)+1) & y+paddery<(length(s)+1)
            if(x-padderx)>0 & (y-paddery)>0
                s(x+padderx,y+paddery) = 0; %Prevent count being
                s(x+padderx,y-paddery) = 0; %counted 2 or more times.
                s(x-padderx,y-paddery) = 0;
                s(x-padderx,y+paddery) = 0;
            end
        end
    end
end
end
end
end
```

